LAWRENCE
LIVERMORE
NATIONAL
LABORATORY

LLNL-JRNL-402058

Evidence and Implications of Frequent Fires in Ancient Shrub Tundra

P. E. Higuera, L. B. Brubaker, P. M. Anderson, T. A. Brown, A. T. Kennedy, F. S. Hu

March 7, 2008

PLoS ONE

Disclaimer

Evidence and Implications of Frequent Fires in Ancient Shrub Tundra

Philip E. Higuera[1,2], Linda B. Brubaker[1], Patricia M. Anderson[3], Thomas A. Brown[4], Alison T. Kennedy[5], Feng Sheng Hu[6]

[1]University of Washington, College of Forest Resources, Seattle, WA 98195

[2]Current affiliations: Montana State University, Department of Earth Sciences, Bozeman, MT 59717; University of Illinois, Department of Plant Biology, Urbana, IL 61801

[3]University of Washington, Department of Earth and Space Sciences and Quaternary Research Center, Seattle, WA 98195

[4]Lawrence Livermore National Laboratory, Center for Accelerator Mass Spectrometry, Livermore, CA, 94551

[5]Montana State University, Department of Earth Sciences, Bozeman, MT 59717

[6]University of Illinois, Department of Plant Biology and Department of Geology, Urbana, IL 61801

Running Head: Implications of Ancient Tundra Fires

Abstract

Understanding feedbacks between terrestrial and atmospheric systems is vital for predicting the consequences of global change, particularly in the rapidly changing Arctic. Fire is a key process in this context, but the consequences of altered fire regimes in tundra ecosystems are rarely considered, largely because tundra fires occur infrequently on the modern landscape. We present paleoecological data that indicate frequent tundra fires in northcentral Alaska between 14,000 and 10,000 years ago. Charcoal and

pollen from lake sediments reveal that ancient birchdominated shrub tundra burned as often as modern boreal forests in the region, every 144 years on average (+/- 90 s.d.; n = 44). Although paleoclimate interpretations and data from modern tundra fires suggest that increased burning was aided by low effective moisture, vegetation cover clearly played a critical role in facilitating the paleo-fires by creating an abundance of fine fuels. These records suggest that greater fire activity will likely accompany temperature-related increases in shrub-dominated tundra predicted for the 21st century and beyond. Increased tundra burning will have broad impacts on physical and biological systems as well as land-atmosphere interactions in the Arctic, including the potential to release stored organic carbon to the atmosphere.

Introduction

Tundra and boreal ecosystems store one third of the world's soil carbon [1]. The fate of this vast carbon stock has become a major concern to global-change scientists because its release to the atmosphere could exacerbate CO_2–related climate change [2-6]. Unfortunately, uncertainty about a number of ecosystem processes hampers predictions of future tundra carbon cycling and the potential consequences to the climate system. One of the most important processes is how vegetation and climate change will alter fire regimes of tundra regions [2,6,7]. Available evidence suggests that ongoing vegetation and climate change could significantly increase the rate of burning in northern tundra [8], which is currently dominated by low-biomass communities (graminoids, herbs, and dwarf shrubs) that seldom burn [e.g. only 3% of Alaskan tundra burned between CE 1950 and 2005; Fig. 1; 9]. In particular, a marked increase in shrub abundance and density, likely resulting from climate warming [10], is changing the physiognomic structure of arctic and subarctic regions. Shrubby growth forms increase the abundance of fine fuels available for burning, and in light of 3-5 °C warming predicted over the next century [8] such fuel changes could result in fire regimes vastly different from those in modern tundra. Unfortunately, short observational fire records [e.g. 48-57 years in Alaska and Canada; 9,11], a lack of fire-history studies, and the possibility of novel future vegetation [12] result in little information to evaluate how tundra fire regimes may respond to future climate

and vegetation change. The paleoecological approach circumvents these limitations and offers the only way to obtain long-term empirical records of fire and vegetation change relevant for understanding tundra fire regimes under future climate and vegetation scenarios.

Here we present fire and vegetation reconstructions from northcentral Alaska that document frequent fires in shrub tundra during the late-glacial and early-Holocene periods (14-10 ka BP [ka BP = thousand years before present, CE 1950]). Vegetation and climate controls of these unusual fire regimes are inferred from paleo-vegetation records from each of two sites and from regional paleo-climate interpretations for this period. We also present an analysis of the climate space occupied by modern tundra vegetation and modern tundra fires in Alaska (CE 1950-2004; Fig. 1). This analysis provides additional support for the climate-fire relationships inferred from the paleo-data.

Results

Trends in charcoal accumulation rates (pieces $cm^{-2}\,yr^{-1}$, CHARs) correspond markedly with shifts in pollen assemblages at Xindi and Ruppert lakes (Fig. 2). Both records start in herb–dominated tundra (Herb Tundra Zone), indicated by high pollen percentages of Cyperaceae (sedge), Poaceae (grass), and minor herb taxa (e.g. *Artemisia* [wormwood], data not shown). Raw CHARs are low (medians = 0.01 and 0.00 pieces $cm^{-2}\,yr^{-1}$) with few identified peaks in the detrended series (Fig. 2), suggesting little or no burning in the late-glacial herb tundra near these sites. Increases in CHARs (medians = 0.05 and 0.02 pieces $cm^{-2}\,yr^{-1}$) and the frequency of peaks in the detrended series coincide with a prominent rise in *Betula* pollen percentages (from < 5 to 50-75%; 14.3 and 13.3 ka BP at Xindi and Ruppert lakes, respectively), which marks the expansion of *Betula* shrubs in the study area (Fig. 2). These pollen assemblages (Shrub Tundra Zone) have higher *Betula* percentages than pollen assemblages from modern tundra in North America [13] (e.g. 70% vs. 40%) and are thought to represent extensive thickets of tall (>1 m) *Betula glandulosa* [resin birch, inferred from measurement of pollen morphology, 14]. The inferred vegetation of the Shrub Tundra Zone contrasts with

modern circumarctic tundra, where only 12% of the area contains shrubs as tall as 0.4 m [i.e. Low-shrub tundra; 15]. However, the vegetation structure of the Shrub Tundra Zone may be analogous to future Arctic tundra, which is predicted to have a major component of > 0.5-m tall *Betula*, *Salix* (willow), and *Alnus* (alder) shrubs [10,16]. Deciduous woodlands (Deciduous Woodland Zone), identified by samples with >10-20 % *Populus* pollen, characterized the vegetation from 10.5-9.0 ka BP (Fig. 2). As in the Herb Tundra Zone, the low raw CHARs (medians = 0.02 and 0.01 pieces cm^{-2} yr^{-1}) and few peaks in the detrended series suggest less frequent fires as compared to the Shrub Tundra Zone.

Estimated fire frequencies within the Shrub Tundra Zone (Figs. 2, 3) were much higher than in modern tundra [9,11] (Fig. 1). Fire events (i.e. CHAR peaks) occurred on average (95% CI) every 171 (134-212) years at Xindi Lake and 137 (107-171) years at Ruppert Lake, with high variability around these means (FRIs range from 30-360 yrs; Fig. 3). FRI distributions at these two lakes were statistically indistinguishable during this period ($p = 0.60$, $n = 24, 20$) and from FRI distributions in late-Holocene boreal forests at Ruppert, Code, and Wild Tussock lakes (p ranges from 0.29-0.99, n ranges from 20-39; Fig. 3)[1]. The fire-vegetation relationships observed at Ruppert and Xindi lakes during the Shrub Tundra Zone are likely regional in scale, as this tundra type is documented in a large network of pollen and macrofossil records in northcentral Alaska [12,13,17], and high fire activity has been qualitatively inferred from discontinuous charcoal records at other sites in interior Alaska [18,19] (Fig. 1b).

Discussion

High fire frequencies in the ancient shrub tundra prompt questions about the relative roles of vegetation (fuels) and climate (summer temperature and precipitation) in controlling fire regimes in the Shrub Tundra Zone and the implications of this natural experiment for understanding future environmental change in the Arctic. Climate is perhaps most often invoked to explain past changes in fire regimes. However, the

[1] Charcoal records from Ruppert, Code, and Wild Tussock lakes for the past 5.5 ka are presented in Supporting Information.

influence of climate on the fire regime in the Shrub Tundra Zone is not straightforward. Near the end of *Betula* shrub dominance and afterwards (ca 11.5-9.0 ka BP), summer temperatures in northern Alaska may have approached or exceeded modern levels [20]. However, such a temperature rise cannot explain the increase in fire frequencies at the beginning of the Shrub Tundra Zone, ca 14.0-12.0 ka BP. In contrast, paleo climate proxies [13] suggest that this period was characterized by cooler-than-present summers. Furthermore, lowered lake levels in interior Alaska indicate effective moisture conditions that were drier than present throughout the Shrub Tundra Zone [21]. Because summer temperatures were cooler than modern, low effective moisture must have been a key factor facilitating the fuel drying necessary to maintain high fire activity within the ancient shrub tundra. The importance of low effective moisture for facilitating tundra burning is evident in the pattern of tundra fires that burned in Alaska between CE 1950-2005. These fires were significantly skewed to tundra regions with relatively dry and/or warm summer climate conditions, i.e. with mean June precipitation between 20-30 mm and mean June temperature between 6-10°C (Fig. 4).

Given our current understanding of the late glaciation and early Holocene, increased burning in the Shrub Tundra Zone was not a simple function of climate change. The distinct increase in CHARs and CHAR peaks at the onset of the Shrub Tundra Zone suggests that vegetation was a key element facilitating fires. The tall growth form, small stem diameters, and highly resinous twigs of *B. glandulosa* [22] make it susceptible to fire on modern landscapes [23], and a widespread cover of *B. glandulosa* in the past would have created the continuity of flammable fuels necessary for fire spread. In addition, vigorous sprouting following fires [23] would have provided the regeneration necessary to sustain fire frequencies similar to those of modern boreal forests (Fig. 3). Based on paleo and modern evidence of tundra fire occurrence and corresponding climatic conditions, the role of fuels is central to understanding past and future shifts in fire regimes. In the case of the Shrub Tundra Zone, the combination of abundant flammable fuels and low effective moisture overwhelmed the mitigating effects of low temperatures on landscape flammability.

Overall, paleo-records from northcentral Alaska imply that ongoing shrub expansion and climate change will result in greater burning within northern tundra ecosystems. The geographic extent of fire-regime changes could be quite large, as shrubs are expected to expand over the next century in both herb and low shrub tundra ecosystems, which comprise 67% of circumpolar Arctic tundra [10,15] (Fig. 1). Over this same period, annual temperatures in the Arctic are projected to increase between 3-5 °C over land, lengthening the growing season and likely decreasing effective moisture (in spite of increased summer precipitation) [8]. How long might it take for the current shrub expansion to trigger a significant change in fire frequencies? Within the chronological limitations of our records, past shrub expansion and fire-regime change occurred within a few centuries (Fig. 2). The duration of this shift is consistent with the estimated rate of shrub expansion within a large area of northern Alaska [0.4% yr-1 for ca 200,000 km^2; 10]. Based on a simple logistic growth model and the assumption of a constant expansion rate, Tape *et al.* [10] hypothesize that the ongoing shrub expansion in this region started roughly 125 years ago and should reach 100% of the region in another 125 years. Thus, if fuels and low effective moisture are major limiting factors for tundra fires, we predict that fire frequencies will increase across modern tundra over the next several centuries.

Although our fire-history records provide unique insights into the potential response of modern tundra ecosystems to climate and vegetation change, they are imperfect analogs for future fire regimes. First, ongoing vegetation changes differ from those of the late-glacial period: several shrub taxa (*Salix*, *Alnus*, and *Betula*) are currently expanding into tundra, whereas *Betula* was the primary constituent of the ancient shrub tundra. The greater flammability of *Betula* compared to *Alnus* and *Salix* could make future shrub tundra less flammable than the ancient shrub tundra. Second, mechanisms of past and future climate change also differ. In the late-glacial and early Holocene periods, Alaskan climate was responding to shrinking continental ice volumes, sealevel changes, and amplified seasonality arising from changes in the seasonal cycle of insolation [13]; in the future, increased concentrations of atmospheric greenhouse gases are projected to cause year-

round arctic warming, but with a greater increase in winter months [8]. Finally, we know little about the potential effects of a variety of biological and physical processes on climate-vegetation-fire interactions. For example, permafrost melting as a result of future warming [8] and/or increased burning [24] could further facilitate fires by promoting shrub expansion [10], or inhibit fires by increasing soil moisture [24].

Despite these uncertainties, Alaskan paleo-records provide clear precedence of shrub-dominated tundra sustaining higher fire frequencies than observed in present-day tundra. The future expansion of tundra shrubs [10,16] coupled with decreased effective moisture [8] could thus enhance circumarctic burning and initiate feedbacks that are potentially important to the climate system. Feedbacks between increased tundra burning and climate are inherently complex [3-5], but studies of modern tundra fires suggest the possibility for both short and long term impacts from (1) increased summer soil temperatures and moisture levels from altered surface albedo and roughness [24], and (2) the release ancient soil carbon through increased permafrost thaw depths and the consumption of the organic layer [24,25]. Given the importance of land-atmosphere feedbacks in the Arctic [26-28], the precedence of a fire-prone tundra biome should motivate further research into the controls of tundra fire regimes and links between tundra burning and the climate system.

Materials and Methods

Lake sediment cores

We reconstructed fire and vegetation history from macroscopic charcoal and palynological data preserved in sediments from four lakes in the southern Brooks Range (Fig. 1b). Ruppert Lake (3 ha; N 67°04’16”, W 154°14’45”; 230 m asl) and Xindi Lake (7 ha; N 67°04’42”, W 152°29’30”; 240 m asl) have records spanning the late-glaciation and early-Holocene (15-9 ka BP). Both sites are surrounded today by boreal forest. Additionally, late-Holocene (last 5.5 ka BP) charcoal records from Ruppert, Code (2 ha; N 67°09’29”, W 151°51’40”; 250 m asl), and Wild Tussock (15 ha; N 67°07’40”, W 151°22’55”; 290 m asl) lakes provide information about fire regimes from modern boreal forest [as defined by 17] for comparison with late-glacial

and earlyHolocene records.

Two parallel, overlapping sediment cores were collected from the center of each lake in summer 2001 (Code), 2002 (Ruppert), and 2003 (Xindi, Wild Tussock) using a modified Livingstonetype piston corer [29] and sliced at 0.25-0.5 cm intervals in the laboratory. Subsamples of 1 cm^3 were prepared at varying intervals for pollen analysis according to PALE protocols [30]. Pollen was counted to a terrestrial pollen sum > 300 at selected levels and assemblages are displayed as percentages of total terrestrial pollen. Pollen zone boundaries, which correspond to pollen zones previously recognized in the region [17], were delineated by visual inspection of pollen percentages of major tree, shrub, and herb taxa. For charcoal analysis, 3-5 cm^3 subsamples were taken from contiguous core slices, soaked in sodium metaphosphate for 72 hours, washed through a 150 μm sieve, and bleached with 8% H_2O_2 for 8 hours. Charcoal was identified at 1040 x magnification based on color, morphology, and texture [31].

Chronologies

Chronologies are based on accelerator mass spectrometry (AMS) ^{14}C-dates of *Betula* (birch) macrofossils, concentrated *Picea* (spruce) pollen grains, and/or concentrated charcoal particles, and all ages are expressed as calibrated ^{14}C year before present[2]. AMS ^{14}C ages were calibrated using CALIB 5.0 and the INTCAL 04 dataset [32]. Calibrated dates and corresponding confidence intervals represent the 50^{th}, 2.5^{th} and 97.5^{th} percentiles of the cumulative probability density function of calibrated ages, respectively [33]. Chronologies were developed using a weighted cubic smoothing spline in Matlab (The MathWorks, Inc.) with the smoothing parameter determined by the average distance (cm) between dates, such that greater sampling resulted in a more flexible spline. The inverse of the 95% confidence interval of the ^{14}C date was used for weighting.

Given the density of radiocarbon dates and that CHARs are sensitive to sedimentation rates, we evaluated

[2] Radiocarbon dates are presented in tabular form in Supporting Information.

whether general features of the CHAR series at both sites varied significantly when using 5-7 alternative age-depth models. In no case did high CHARs or the distinct peaks of the Shrub Tundra Zone disappear. Charcoal concentrations (pieces cm^{-3}) are also high in this period, giving us confidence that the high CHARs reflect increased charcoal accumulation and are not chronological artifacts.

Statistical treatment of charcoal data

Peaks in the charcoal accumulation rate (pieces cm^{-2} yr^{-1}; CHAR) in lake sediment have been shown both empirically [34] and through mechanistic models [35] to be associated with the local (0.5-1.0 km) occurrence of individual or multiple high-severity fires ("fire events"). Local fires introduce charcoal to a lake via airborne fallout and create distinct CHAR peaks that exceed variability around a long-term trend. This characteristic can be taken advantage of in many charcoal records to infer when local fires occurred in the past. We estimated the timing of fire events in our charcoal records by removing low-frequency trends (reflecting changes in the rates of charcoal production, secondary transport, sediment mixing, and sediment sampling) and applying a locally-defined threshold value that separates fire-related CHAR peaks ("signal") from non-fire-related variability in CHARs ("noise"). Our approach accounts for both changes in the mean and variance in charcoal accumulation through time and the statistical nature of charcoal counts.

Prior to quantitative analysis, charcoal data were interpolated to constant 15-yr time steps, approximating the median temporal resolution of each record. Low-frequency trends in CHARs, Clow-frequency, were estimated by the 500-yr running median, smoothed with locally-weighted regression (also with a 500-yr window). We subtracted $C_{low\text{-}frequency}$ from the raw charcoal series to obtain a residual "peak" series, C_{peak}. For each record, we selected a threshold value t that identifies charcoal peaks when $C_{peak} > t$. Our threshold criterion assumes that fires create charcoal peaks that exceed C_{peak} variations related to sediment mixing, sediment sampling, and analytical noise, and that this variability changes on time scales > 500 years. Thus, for each 500yr period, we assume that the distribution of C_{peak} values contains two sub-populations, C_{noise}

and C_{fire}. C_{noise} is a normally distributed population centered near 0 (i.e. $C_{low\text{-}frequency}$); C_{fire} samples are the high CHARs caused by local fires and consist of positive C_{peak} values exceeding the variation in C_{noise}. We used a Gaussian mixture model to identify the mean and variance of the C_{noise} distribution [36] and used the 99th percentile of this distribution as the threshold value. For all records, this procedure was done for each overlapping 500-yr period, producing a unique threshold for each sample. Individual thresholds for each sample were smoothed with a locallyweighted regression (to 500 yr). Finally, all peaks exceeding the locally-defined threshold were screened based on the original charcoal counts contributing to each peak. If the maximum count contributing to a CHAR peak had a > 5% chance of coming from the same Poisson-distributed population as the minimum charcoal count within the proceeding 75 years, then the "peak" was not identified [e.g. Charster user's guide, accessed September 2007, http://geography.uoregon.edu/gavin/charster/Analysis.html; 37]. Our charcoal analysis methods are contained within the program *CharAnalysis*, written by PEH and available online at http://CharAnalysis.googlepages.com.

Quantifying fire regimes

We used dates of estimated fire events to calculate fire return intervals (years between fire events; FRIs) and fit a two-parameter Weibull model to the distribution of FRIs within each vegetation zone using maximum likelihood techniques [38]. Each Weibull model passed a Kolmogorov-Smirnov goodness-of-fit-test ($p > 0.10$), and we estimated 95% confidence intervals for the Weibull scale, *b,* and shape, *c*, parameters based on 1000 bootstrapped samples from each population. Confidence intervals for the mean FRI were calculated in the same manner.

We used a likelihood ratio test, based on likelihood values of the Weibull model fit to the FRI data, to test the null hypothesis that two FRI distributions were similar [38,39]. The probability of Type I Error, p, was estimated using a permutation test, and the null hypothesis was rejected if $p < 0.05$.

Climate space of modern tundra and tundra fires

The climate space occupied by modern tundra vegetation and tundra fires was quantified using tundra classification data from the Circumpolar Arctic Vegetation Map [15], temperature and precipitation data from the Global Historical Climatology Network [W. Cramer, W. University of California-Berkeley/Integrative Biology and U.S. Geological Survey/Alaska Geographic Science Office. (2006) accessed on-line in January 2007: http://agdc.usgs.gov/data/projects/hlct/hlct.html#A], and area burned data from the Alaska Fire Service [accessed on-line in January 2007: http://agdc.usgs.gov/data/blm/fire/index.html]. Each dataset was imported into a raster-based geographic information system with a 1 km^2 cell size. Climate space was determined based on the average June precipitation and average June temperature values from all cells with: (1) CAVM classification of tundra, and (2) burned cells with a CAVM classification of tundra.

Acknowledgements

Sampling was conduced under permit from Gates of the Arctic National Park and the Bureau of Land Management. We thank B. Clegg, J. Mauro, and K. Shick, for field assistance, Brooks Range Aviation and VECO Polar Resources for field logistics, C. Adam, E. Cudaback, J. Leach, A. Lilienthal (Yambor), J. Smith, and E. Spaulding for laboratory assistance, and C. Whitlock, C. Carcaillet, and two anonymous reviewers for constructive comments on the manuscript. This work was performed in part under the auspices of the U.S. Department of Energy by Lawrence Livermore National Laboratory in part under Contract W-7405-Eng-48 and in part under Contract DE-AC52-07NA27344.

Author Contributions

PEH, LBB, and FSH designed and conducted field work. PEH and LBB oversaw lab work and PEH

designed and performed data analyses. LBB and PMA counted pollen from Ruppert and Xindi lakes, respectively. TAB oversaw ^{14}C dating and assisted in chronology development. ATK gathered and summarized the data presented in Fig. 4. PEH wrote the paper with significant input from LBB, FSH, and PMA.

Funding

Research was supported by grants from the National Science Foundation's Graduate Research Fellowship (to PEH) Arctic System Science (to LBB, PMA, and TB) programs.

Competing Interests

The authors declare no competing interests.

References

1. Post WM, Emanuel WR, Zinke PJ, Stangenberger AG (1982) Soil Carbon Pools and World Life Zones. Nature 298: 156-159.

2. Chapin FS, McGuire AD, Randerson J, Pielke RS, Baldocchi D, et al. (2000) Arctic and boreal ecosystems of western North America as components of the climate system. Global Change Biology 6: 211-223.

3. Shaver GR, Giblin AE, Nadelhoffer KJ, Thieler KK, Downs MR, et al. (2006) Carbon turnover in Alaskan tundra soils: effects of organic matter quality, temperature, moisture and fertilizer. Journal of Ecology 94: 740-753.

4. Oechel WC, Vourlitis GL, Hastings SJ, Zulueta RC, Hinzman L, et al. (2000) Acclimation of ecosystem CO_2 exchange in the Alaskan Arctic in response to decadal climate warming. Nature 406: 978-981.

5. Mack MC, Schuur EAG, Bret-Harte MS, Shaver GR, Chapin FS (2004) Ecosystem carbon storage in arctic tundra reduced by long-term nutrient fertilization. Nature 431: 440-443.

6. Sitch S, McGuire AD, Kimball J, Gedney N, Gamon J, et al. (2007) Assessing the carbon balance of circumpolar Arctic tundra using remote sensing and process modeling. Ecological Applications 17: 213-234.

7. Bond-Lamberty B, Peckham SD, Ahl DE, Gower ST (2007) Fire as the dominant driver of central Canadian boreal forest carbon balance. Nature 450: 89-+.

8. ACIA (2004) Impacts of a Warming Arctic: Arctic Climate Impact Assessment. Cambridge: Cambridge University Press. 1042 p.

9. Kasischke ES, Williams D, Barry D (2002) Analysis of the patterns of large fires in the boreal forest region of Alaska. International Journal of Wildland Fire 11: 131-144.

10. Tape K, Sturm M, Racine C (2006) The evidence for shrub expansion in Northern Alaska and the Pan-Arctic. Global Change Biology 12: 686-702.

11. Stocks BJ, Mason JA, Todd JB, Bosch EM, Wotton BM, et al. (2002) Large forest fires in Canada, 1959-1997. Journal of Geophysical Research-Atmospheres 108.

12. Edwards ME, Brubaker LB, Lozhkin AV, Anderson PM (2005) Structurally novel biomes: a response to past warming in Beringia. Ecology 86: 1696-1703.

13. Anderson PM, Edwards ME, Brubaker LB (2004) Results and paleoclimate implications of 35 years of paleoecological research in Alaska. Developments in Quaternary Science 1: 427340 440.

14. Brubaker LB, Garfinkel HL, Edwards ME (1983) A late Wisconsin and Holocene vegetation history from the central Brooks Range: Implications for Alaskan paleoecology. Quaternary Research 20: 194-214.

15. Walker DA, Raynolds MK, Daniels FJA, Einarsson E, Evlvebakk A, et al. (2005) The circumpolar Arctic vegetation map. Journal of Vegetation Science 16: 267-282.

16. Walker MD, Wahren CH, Hollister RD, Henry GHR, Ahlquist LE, et al. (2006) Plant community responses to experimental warming across the tundra biome. Proceedings of the National Academy of Sciences of the United States of America 103: 1342-1346.

17. Anderson PM, Brubaker LB (1994) Vegetation history of northcentral Alaska: a mapped summary of Late-Quaternary pollen data. Quaternary Science Reviews 13: 71-92.

18. Tinner W, Hu FS, Beer R, Kaltenrieder P, Scheurer B, et al. (2006) Postglacial vegetational and fire history: pollen, plant macrofossil and charcoal records from two Alaskan lakes. Vegetation History and Archaeobotany 15: 279-293.

19. Earle CJ, Brubaker LB, Anderson PM (1996) Charcoal in northcentral Alaskan lake sediments: relationships to fire and late-Quaternary vegetation history. Review of Paleobotany and Palynology 92: 83-95.

20. Kaufman DS, Ager TA, Anderson NJ, Anderson PM, Andrews JT, et al. (2004) Holocene thermal maximum in the western Arctic (0-180 degrees W). Quaternary Science Reviews 23: 529-560.

21. Abbott MB, Finney BP, Edwards ME, Kelts KR (2000) Lake-level reconstruction and paleohydrology of Birch Lake, central Alaska, based on seismic reflection profiles and core transects. Quaternary Research 53: 154-166.

22. Dugle JR (1966) A taxonomic study of Western Canadian species in genus *Betula*. Canadian Journal of Botany 44: 929-&.

23. de Groot WJ, Wein RW (1999) *Betula glandulosa* Michx. response to burning and postfire growth temperature and implications of climate change. International Journal of Wildland Fire 9: 51-64.

24. Liljedahl A, Hinzman L, Busey R, Yoshikawa K (2007) Physical short-term changes after a tussock tundra fire, Seward Peninsula, Alaska. Journal of Geophysical Research-Earth Surface 112.

25. Racine C, Allen JA, Dennis JG (2006) Long-term monitoring of vegetation change following tundra fires in Noatak National preserve, Alaska. Arctic Network of Parks Inventory and Monitoring Program, National Park Service, Alaska Region. NPS/AKRARCN/NRTR 2006/02
NPS/AKRARCN/NRTR-2006/02
37 p.

26. Zimov SA, Schuur EAG, Chapin FS (2006) Permafrost and the Global Carbon Budget. Science 32: 1612-1613.

27. McGuire AD, Chapin FS, Walsh JE, Wirth C (2006) Integrated regional changes in arctic climate

feedbacks: Implications for the global climate system. Annual Review of Environment and Resources 31: 61-91.

28. Eugster W, Rouse WR, Pielke RAS, McFadden JP, Baldocchi DD, et al. (2000) Landatmosphere energy exchange in Arctic tundra and boreal forest: available data and feedbacks to climate. Global Change Biology 6: 84-115.

29. Wright HE, Mann DH, Glaser PH (1984) Piston corers for peat and lake sediments. Ecology 65: 657-659.

30. PALE_members (1994) Research Protocols for PALE: Paleoclimates of Arctic Lakes and Estuaries. PAGES workshop report: 53.

31. Rhodes AN (1998) A method for the preparation and quantification of microscopic charcoal from terrestrial and lacustrine sediment cores. The Holocene 8: 113-117.

32. Reimer PJ, Baillie MGL, Bard E, Bayliss A, Beck JW, et al. (2004) INTCAL04 terrestrial radiocarbon age calibration, 0-26 cal Kyr BP. Radiocarbon 46: 1029-1058.

33. Telford RJ, Heegaard E, Birks HJB (2004) The intercept is a poor estimate of a calibrated radiocarbon age. The Holocene 14: 296-298.

34. Lynch JA, Clark JS, Stocks BJ (2004) Charcoal production, dispersal and deposition from the Fort Providence experimental fire: Interpreting fire regimes from charcoal records in boreal forests. Canadian Journal of Forest Research 34: 1642-1656.

35. Higuera PE, Peters ME, Brubaker LB, Gavin DG (2007) Understanding the origin and analysis of sediment-charcoal records with a simulation model. Quaternary Science Reviews 26: 1790-1809.

36. Gavin DG, Hu FS, Lertzman K, Corbett P (2006) Weak climatic control of stand-scale fire history during the late Holocene. Ecology 87: 1722-1732.

37. Shiue W, K., Bain LJ (1982) Experiment size and power comparisons for two-sample Poission tests. Journal of Applied Statistics 31: 130-134.

38. Johnson EA, Gutsell SL (1994) Fire frequency models, methods and interpretations. Advances in

Ecological Research 25: 239-287.

39. Thoman DR, Bain LJ (1969) Two sample tests in the Weibull distribution. Technometrics 11: 805-815.

Figure Captions

Figure 1. (a) Distribution of modern circumpolar Arctic tundra [15]. Black rectangles indicate regions showing increases in modern shrub densities and/or extent [10]. (b) Alaskan fires from 1950-2005 (red polygons) in tundra and boreal forest. Fires occurred in only 3% percent of Alaskan tundra, representing 6% of the total area burned in the state. Blue dots identify study lakes: Ruppert (RP), Xindi (XI), Code (CO), and Wild Tussock (WK). Charcoal from Sithylemenkat Lake [19] (1) and Lost Lake [18] (2) also show qualitative evidence of increased fire activity within the Shrub Tundra Zone.

Figure 2: Chronology, pollen stratigraphy, inferred vegetation, and high-frequency variations in charcoal accumulation rates (CHARs) for (a) Xindi Lake and (b) Ruppert Lake. Pollen percentage curves are smoothed to 500 years and color coded. CHAR records represent residuals after removing 500-year trends. Red lines around CHAR = 0 are thresholds identifying noiserelated variations in CHARs; red plus marks identify CHAR peaks exceeding this noise-related threshold and are interpreted as local fire events. CHARs and CHAR peaks increase distinctly with the rise in *Betula* pollen percentages, marking the transition from the Herb Tundra Zone to the Shrub Tundra Zone.

Figure 3: Fire return intervals (FRIs) from the Shrub Tundra Zone at (a) Xindi and (b) Ruppert lakes with Weibull models (blue lines). Weibull *b* (yr) and *c* (unitless) parameters, and the mean FRI (mFRI; yr) all include 95% confidence intervals. (c) Weibull models from the Shrub Tundra Zone (blue solid lines) and the conifer-dominated Boreal Forest Zone (black dashed lines). The Weibull *b* and *c* parameters, and mFRI for Ruppert (boreal forest), Code, and Wild Tussock lakes are 188 (147-239), 150 (123-178), and 149 (123-174); 1.53 (1.31-2.06), 1.85 (1.52-2.60), and 1.96 (1.61-2.75); 171 (135-216), 135 (113-160), and 135 (113-

157).

Figure 4: Climate space occupied by all Alaskan tundra in the circumpolar Arctic vegetation map [15] (CAVM, gray) and area burned (red) within the same region from CE 1950-2005. Darker colors represent a greater proportion of total tundra vegetation (gray) or total area burned (red) within the climate space. Mean June temperature and precipitation distributions associated with tundra vegetation and area burned are shown as histograms and box plots. For both temperature and precipitation, distributions for vegetation and area burned differ significantly based on a Kolmogorov Smirnov test with $N_{fires} = 232$ degrees of freedom ($p < 0.01$).

Figure 1.

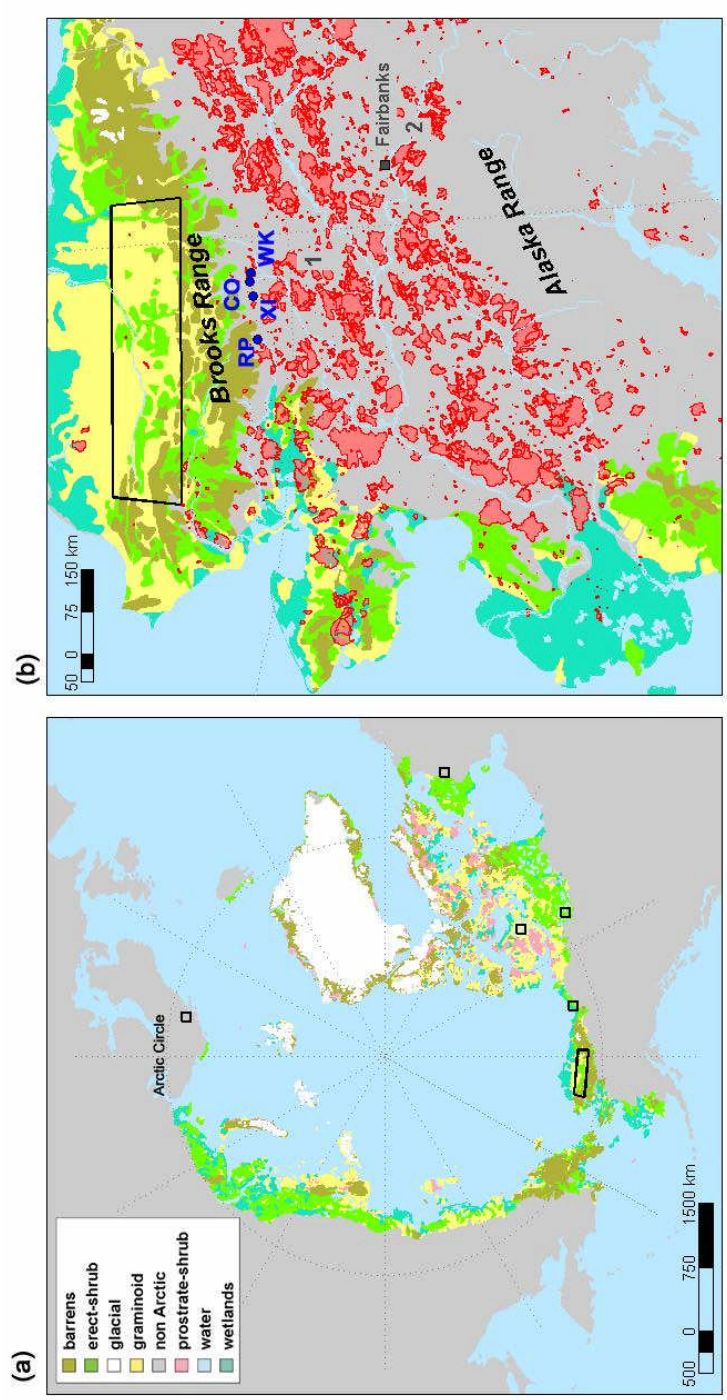
(a)
barrens
erect-shrub
glacial
graminoid
non Arctic
prostrate-shrub
water
wetlands
Arctic Circle
500 0 750 1500 km
(b)
50 0 75 150 km
Brooks Range
CO
RP
XL
WK
1
2
Fairbanks
Alaska Range

Figure 2.

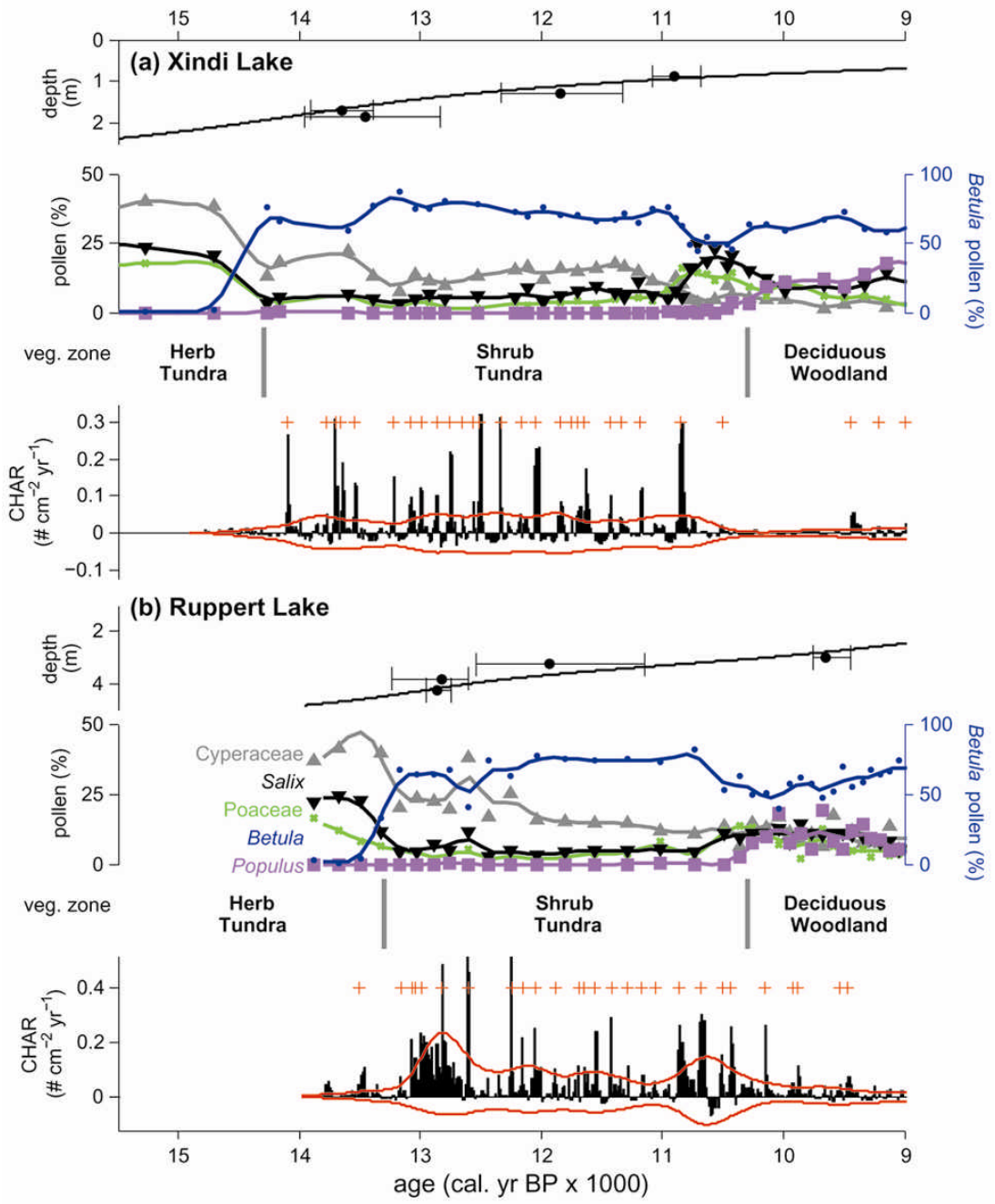
(a) Xindi Lake
depth (m)
pollen (%)
Betula pollen (%)
veg. zone
Herb Tundra
Shrub Tundra
Deciduous Woodland
CHAR (# cm−2 yr−1)
(b) Ruppert Lake
Cyperaceae
Salix
Poaceae
Betula
Populus
age (cal. yr BP x 1000)

Figure 3.

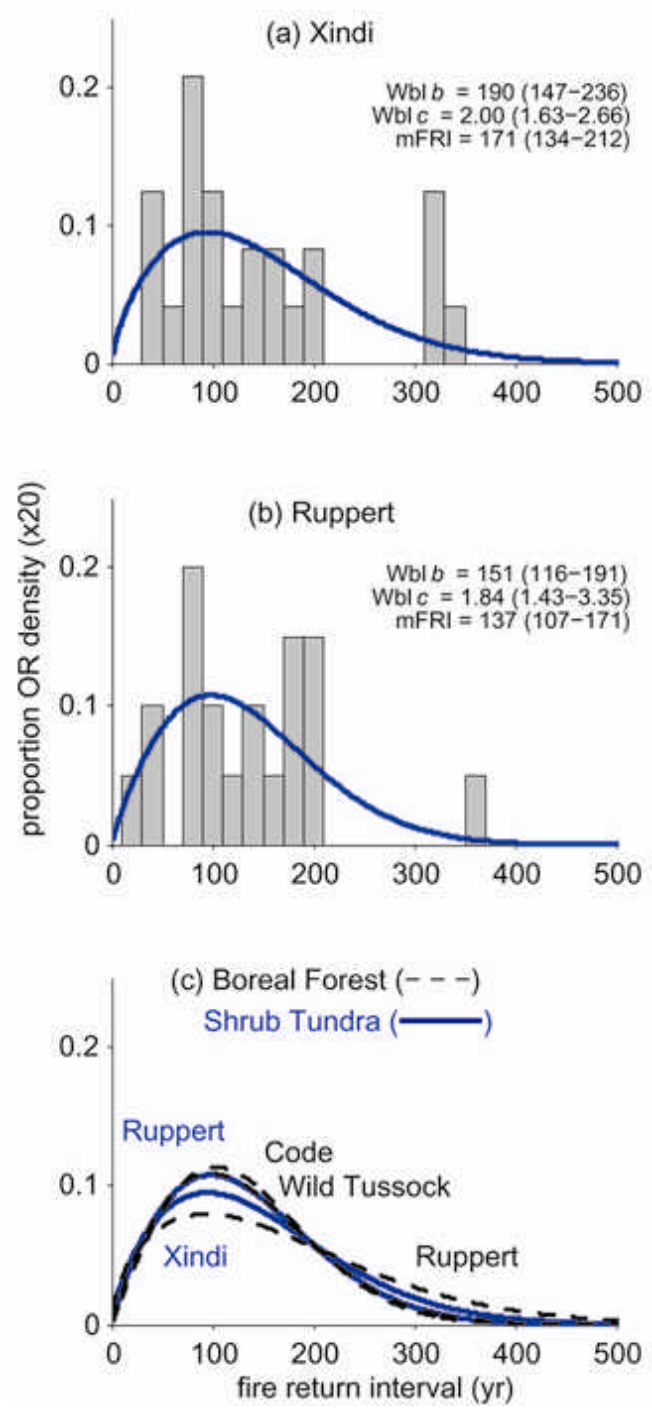
(a) Xindi
Wbl b = 190 (147–236)
Wbl c = 2.00 (1.63–2.66)
mFRI = 171 (134–212)
(b) Ruppert
Wbl b = 151 (116–191)
Wbl c = 1.84 (1.43–3.35)
mFRI = 137 (107–171)
proportion OR density (x20)
(c) Boreal Forest (– – –)
Shrub Tundra (——)
Ruppert
Code
Wild Tussock
Xindi
Ruppert
fire return interval (yr)

Figure 4.

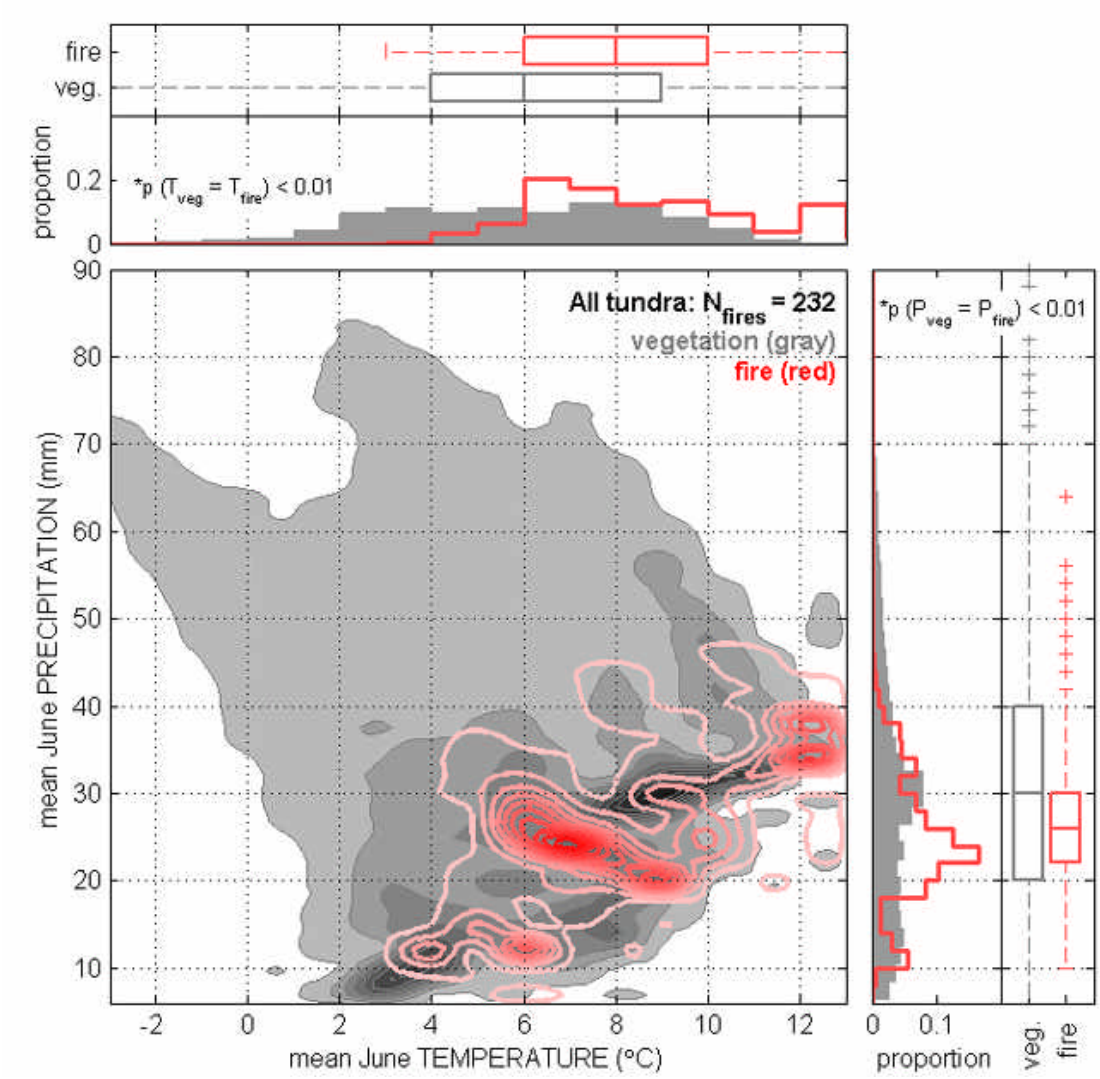
fire
veg.
proportion
0.2
0
*p (T_veg = T_fire) < 0.01
All tundra: N_fires = 232
vegetation (gray)
fire (red)
*p (P_veg = P_fire) < 0.01
mean June PRECIPITATION (mm)
90
80
70
60
50
40
30
20
10
-2
0
2
4
6
8
10
12
mean June TEMPERATURE (°C)
0
0.1
proportion
veg.
fire

Supporting Information

Table S1. Radiocarbon dates and calibrated ages for Ruppert, Xindi, Code, and Wild Tussock lakes.

Sample depth (cm)	Material Dated	Laboratory ID[1]	^{14}C date[2] (yr BP)	Calibrated date[3]	95% CI
Ruppert Lake					
16.60 - 17.60	concentrated charcoal	CAMS 106161	600 ± 100	594	475 - 743
26.48 - 27.20	concentrated charcoal	CAMS 110400	1170 ± 35	1088	1002 - 1190
30.5 - 31.5	concentrated charcoal	CAMS 106160	1150 ± 60	1065	904 - 1175
41.17 - 42.13	concentrated charcoal	CAMS 111400	1505 ± 40	1388	1266 - 1461
45.98 - 46.71	concentrated charcoal	CAMS 110401	1740 ± 35	1648	1542 - 1739
57.78 - 58.75	con. charcoal & *Picea* needle	CAMS 111401	2185 ± 40	2210	2104 - 2352
78.5 - 79.5	concentrated charcoal	CAMS 110948	3000 ± 60	3185	3029 - 3379
86.5 - 87.0	concentrated charcoal	CAMS 111402	3145 ± 35	3369	3285 - 3466
99.0 - 100.0	concentrated *Picea* pollen	CAMS 100063	3860 ± 45	4281	4155 - 4429
100.0 - 101.0	con. charcoal & *Picea* needle	CAMS 110949	3770 ± 40	4137	4004 - 4275
115.2 - 115.6	concentrated charcoal	CAMS 110402	5050 ± 45	5812	5720 - 5952
160.5 - 161.0	concentrated charcoal	CAMS 110950	6350 ± 110	7266	7077 - 7556
206.5 - 207.5	concentrated charcoal	CAMS 113762	7460 ± 110	8256	8082 - 8478
298.0 - 300.5	con. charcoal & *Betula* leafs	CAMS 122361	8710 ± 40	9654	9446 - 9750
324.5 - 326.5	concentrated charcoal	CAMS 111403	10220 ± 160	11939	11159 - 12549
380.5 - 381.5	concentrated charcoal	CAMS 110951	10740 ± 80	12820	12610 - 13239
423.9 - 427.4	concentrated charcoal	CAMS 122362	10870 ± 80	12860	12749 - 12952
Xindi Lake					
10.5 - 12.0	concentrated charcoal	CAMS 113558	1240 ± 70	1159	1036 - 1323
24.0 - 25.5	concentrated charcoal	CAMS 116226	3490 ± 35	3956	3940 - 3963
31.0 - 32.0	concentrated *Picea* pollen	CAMS 105876	4930 ± 90	5679	5472 - 5877
32.0 - 33.0	concentrated charcoal	CAMS 112145	4560 ± 120	5208	4860 - 5527
43.0 - 43.5	concentrated charcoal	CAMS 113559	4760 ± 70	5493	5377 - 5656
51.0 - 52.0	concentrated charcoal	CAMS 116227	5960 ± 60	7153	7144 - 7156
85.5 - 87.5	wood macrofossil	CAMS 106159	9585 ± 40	10907	10685 - 11083
127.0 - 127.5	concentrated charcoal	CAMS 114331	10180 ± 120	11844	11332 - 12330
167.5 - 168.5	concentrated charcoal	CAMS 114332	11800 ± 120	13648	13391 - 13903
183.5 - 184.5	concentrated charcoal	CAMS 114333	11570 ± 300	13456	12833 - 13961
Code Lake					
8.50 - 9.00	concentrated charcoal	CAMS 116841	405 ± 40	534	513 - 537
31.00 - 31.50	concentrated charcoal	CAMS 114723	1295 ± 35	1235	1182 - 1325
49.00 - 49.50	concentrated charcoal	CAMS 114724	2275 ± 30	2305	2266 - 2443
59.25 - 60.00	concentrated charcoal	CAMS 116840	2805 ± 40	3154	3104 - 3167
86.25 - 87.00	wood macrofossil	CAMS 80792	4155 ± 40	4691	4560 - 4833
96.50 - 97.50	concentrated charcoal	CAMS 116839	4875 ± 35	5742	5630 - 5746
123.00 - 123.50	wood macrofossil	CAMS 80794	6555 ± 40	7462	7367 - 7552
Wild Tussock Lake					
31.00 - 31.25	concentrated charcoal	CAMS 112143	1895 ± 45	1845	1737 - 1955
53.25 - 53.75	concentrated charcoal	CAMS 113763	2880 ± 60	3012	2820 - 3167
69.25 - 70.75	concentrated charcoal	CAMS 122363	3360 ± 35	3601	3516 - 3714
116.00 - 116.50	concentrated charcoal	CAMS 112144	4920 ± 70	5671	5461 - 5831
111.75 - 113.75	concentrated charcoal	CAMS 116228	4590 ± 50	5578	5572 - 5580
132.75 - 133.50	concentrated charcoal	CAMS 116229	5660 ± 120	6991	6833 - 7013

[1]CAMS: Center for Accelerator Mass Spectrometry, Lawrence Livermore National Laboratory, Livermore, CA.

[2]Conventional radiocarbon years before present (CE 1950) and standard deviation. [3]See Methods.

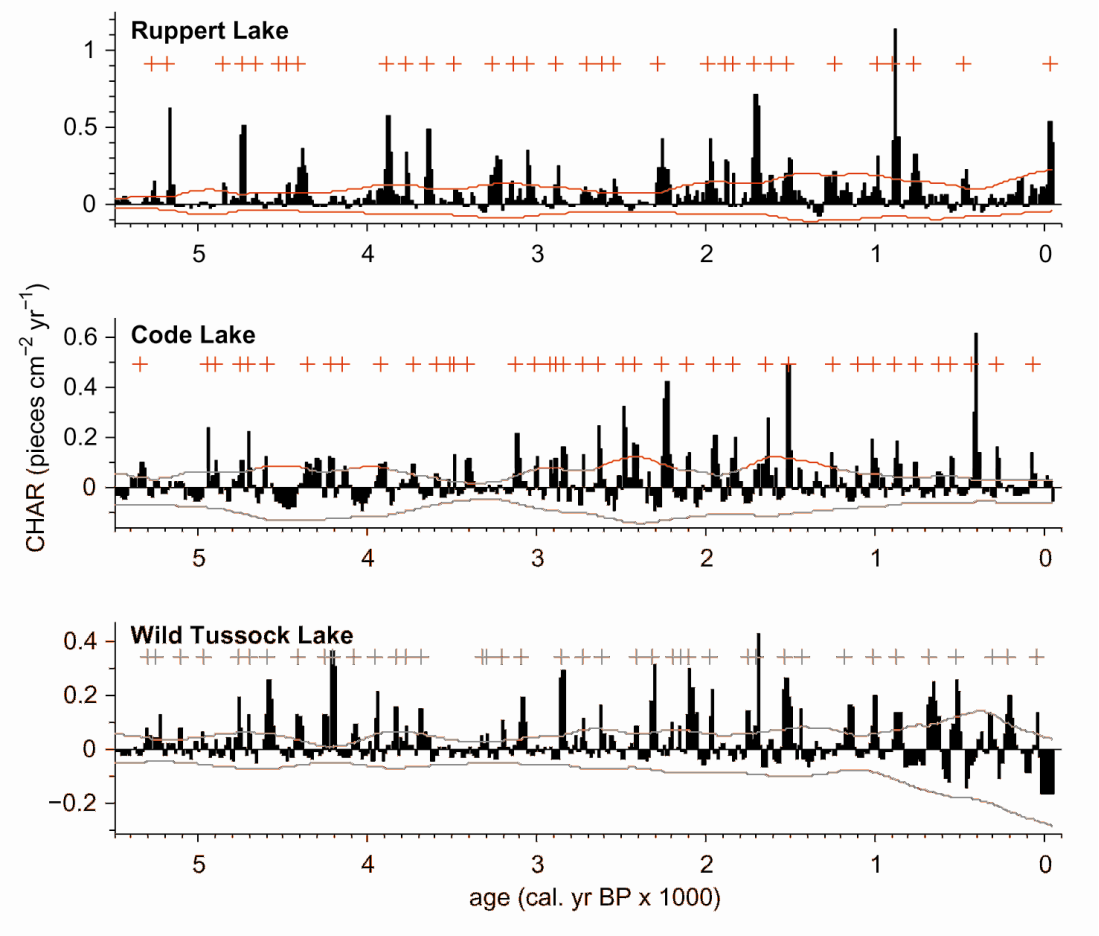

Figure S1. High-frequency trends in the charcoal accumulation rate (CHAR), C_{peak}, within the Boreal Forest Zone (5.5 ka BP – present) at Ruppert, Code, and Wild Tussock lakes. Red lines represent modeled variations in C_{noise}, and plus marks identify peaks interpreted as local fire events. See Methods and Materials for details.